Involvement of Individual Subsites and Secondary Substrate Binding Sites in Multiple Attack on Amylose by Barley α-Amylase†

Birte Kramhøft,‡,§ Kristian Sass Bak-Jensen,‡,|| Haruhide Mori,‡,⊥ Nathalie Juge,▽ Jane Nøhr,∞ and Birte Svensson*,‡,§

Department of Chemistry, Carlsberg Laboratory, Gamle Carlsberg Vej 10, DK-2500 Copenhagen Valby, Denmark, Biochemistry and Nutrition Group, BioCentrum-DTU, Technical University of Denmark, Søltofts Plads, Building 224, DK-2800 Kgs. Lyngby, Denmark, Institute of Food Research, Norwich Research Park, Colney, Norwich, NR4 7UA, England, and Department of Biochemistry and Molecular Biology, University of Southern Denmark, Campusvej 55, DK-5230 Odense M, Denmark

Received September 3, 2004; Revised Manuscript Received December 3, 2004

ABSTRACT: Barley α-amylase 1 (AMY1) hydrolyzed amylose with a degree of multiple attack (DMA) of 1.9; that is, on average, 2.9 glycoside bonds are cleaved per productive enzyme−substrate encounter. Six AMY1 mutants, spanning the substrate binding cleft from subsites −6 to +4, and a fusion protein, AMY1−SBD, of AMY1 and the starch binding domain (SBD) of *Aspergillus niger* glucoamylase were also analyzed. DMA of the subsite −6 mutant Y105A and AMY1−SBD increased to 3.3 and 3.0, respectively. M53E, M298S, and T212W at subsites −2, +1/+2, and +4, respectively, and the double mutant Y105A/T212W had decreased DMA of 1.0−1.4. C95A (subsite −5) had a DMA similar to that of wild type. Maltoheptaose (G7) was always the major initial oligosaccharide product. Wild-type and the subsite mutants released G6 at 27−40%, G8 at 60−70%, G9 at 39−48%, and G10 at 33−44% of the G7 rate, whereas AMY1−SBD more efficiently produced G8, G9, and G10 at rates similar to, 66%, and 60% of G7, respectively. In contrast, the shorter products appeared with large individual differences: G1, 0−15%; G2, 8−43%; G3, 0−22%; and G4, 0−11% of the G7 rate. G5 was always a minor product. Multiple attack thus involves both longer translocation of substrate in the binding cleft upon the initial cleavage to produce G6−G10, essentially independent of subsite mutations, and short-distance moves resulting in individually very different rates of release of G1−G4. Accordingly, the degree of multiple attack as well as the profile of products can be manipulated by structural changes in the active site or by introduction of extra substrate binding sites.

Enzymes such as different starch-degrading enzymes, pectinases, cellulases, endo- and exonucleases, that catalyze the hydrolysis of polymers, have been found to act by a mechanism in which several substrate bonds are cleaved without dissociation of the enzyme−polymer complex (*1*−*7*). This mode of action was denoted multiple attack as described first for *β*-amylase (*1*) specifically releasing maltose from nonreducing ends of α-1,4-glucans (*4*). The concept was subsequently applied to α-amylases (*2*, *4*, *8*, *9*), and the degree of multiple attack (DMA) was defined as the number of bonds hydrolyzed succeeding the initial cleavage in a single enzyme−substrate encounter (*2*). The multiple attack mechanism thus represents an intermediate of the "single-chain" and the "multi-chain" mechanisms (*2*). In the former, a polymer molecule is hydrolyzed to completion by the productive enzyme−substrate complex, whereas the latter involves classical random attack, in which only one substrate bond is hydrolyzed per productive complex. DMA among α-amylases varies, being 6 for porcine pancreatic α-amylase (PPA), 3 for human salivary α-amylase, and 2 for both TAKA amylase from *Aspergillus oryzae* (*2*) and an alkalophilic α-amylase from *Bacillus* (*9*), while

† This work was supported by the EU Third and Fourth Framework Programs on Biotechnology to the projects NEWAMASE (CT94-3008) and AGADE (CT98-0022), and the Danish Research Council's Committee on Biotechnology (Grant 9502014).

* To whom correspondence should be addressed. Permanent address: Biochemistry and Nutrition Group, BioCentrum-DTU, Technical University of Denmark, Søltofts Plads, Building 224, DK-2800 Kgs. Lyngby, Denmark. Phone +45 4525 2740; fax +45 4588 6307; e-mail bis@biocentrum.dtu.dk.

‡ Carlsberg Laboratory.

§ Technical University of Denmark.

|| Present address: DNAX Research Inc., 901 California Ave., Palo Alto, CA 94304.

⊥ Present address: Division of Applied Bioscience, Graduate School of Agriculture, Hokkaido University, Sapporo 060-8589, Japan.

▽ Institute of Food Research, Norwich.

∞ University of Southern Denmark. Present address: Invitrogen A/S, Thistedgade 6, DK-2630 Taastrup, Denmark.

[1] Abbreviations: AMY1, low p*I* barley α-amylase; AMY2, high p*I* barley α-amylase; BSA, bovine serum albumin; DMA, degree of multiple attack; DMSO, dimethyl sulfoxide; DP, degree of polymerization; G1, glucose; G2, maltose; G3, maltotriose; G4, maltotetraose; G5, maltopentaose; G6, maltohexaose; G7, maltoheptaose; G8, maltooctaose; G9, maltononaose; G10, maltodecaose; G11−G25, linear maltooligosaccharides of degree of polymerization 11−25; GH13, glycoside hydrolase family 13; HPAEC−PAD, high-performance anion-exchange chromatography with pulsed amperometric detection; PPA, porcine pancreatic α-amylase; RV_t, rate of total reducing product formation; RV_p, rate of ethanol-insoluble reducing product formation; RV_s, rate of ethanol-soluble reducing product formation; SBD, starch binding domain; TCA, trichloroacetic acid.

10.1021/bi048100v CCC: $30.25
Published on Web 01/22/2005

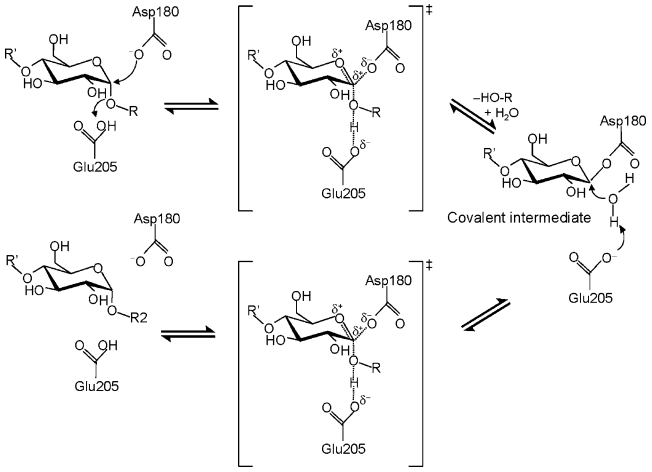

FIGURE 1: Catalytic mechanism of retaining glycosidases. In hydrolysis the covalent intermediate is attacked at C1 by H_2O, leading to a second transition state, followed by release of product.

preliminary analysis of barley α-amylase gave a DMA of about 1 (*9*). The term processivity was later introduced to describe multiple attack for other polysaccharide hydrolases such as cellulases (*5*, *10*, *11*), chitinases (*12*), and pectinases (*6*). DMA of 2−7 was reported for endocellulases from *Thermospora fusca* and up to 20 for exoacting cellulases from *T. fusca* and *Trichoderma reesei* (*10*).

In general, cleft-shaped binding sites are found in endo-acting carbohydrases (*7*, *11*, *13*, *14*), whereas exo-acting carbohydrases, such as exo-acting cellulases, can have a tunnel-shaped binding site (see *11*). In both cases the active site is composed of an array of subsites, each of which interacts with individual sugar residues of the substrate. Some starch-degrading enzymes possess in addition distinct surface or secondary binding sites (*13*, *15*−*17*), participating possibly in the degradation of polymeric substrates (*11*, *18*). Structural details of molecular events in multiple attack are largely unknown. However, crystallography on different oligosaccharide complexes of the cellobiohydrolase Cel6A from *Humicola insolens* proposed characteristics of the change in enzyme−substrate interactions near the catalytic site during processive action. In this work, snapshots of a variety of ligands in different positions depict substrate movements as facilitated by solvent-mediated interactions and flexible hydrophobic contacts generated by a sheet of tryptophans in the binding site (*19*).

The present study focuses on the role of the structure of the barley α-amylase substrate-binding site in multiple attack on amylose. α-Amylases (α-1,4-D-glucan glucanohydrolase, EC 3.2.1.1) hydrolyze internal α-1,4-glucoside linkages in starch and related poly- and oligosaccharides. They belong to glucoside hydrolase family 13 (GH13) (*20*, *21*) sharing three structural domains: a catalytic $(\beta/\alpha)_8$-barrel (domain A) with a long $\beta \rightarrow \alpha$ loop (domain B) protruding at the third β-strand, followed by a C-terminal β-sheet domain (domain C) (*22*). The substrate is accommodated in a cleft between domains A and B (see ref *23*) that in different α-amylases has from 5 to 11 consecutive subsites binding substrate glycosyl residues (*24*−*26*). A two-step double displacement catalytic mechanism (Figure 1; *20*) leads to retention of the anomeric configuration of the substrate after hydrolysis. First the acid/base catalyst protonates the glucosidic oxygen of the bond to be cleaved, then via a transition

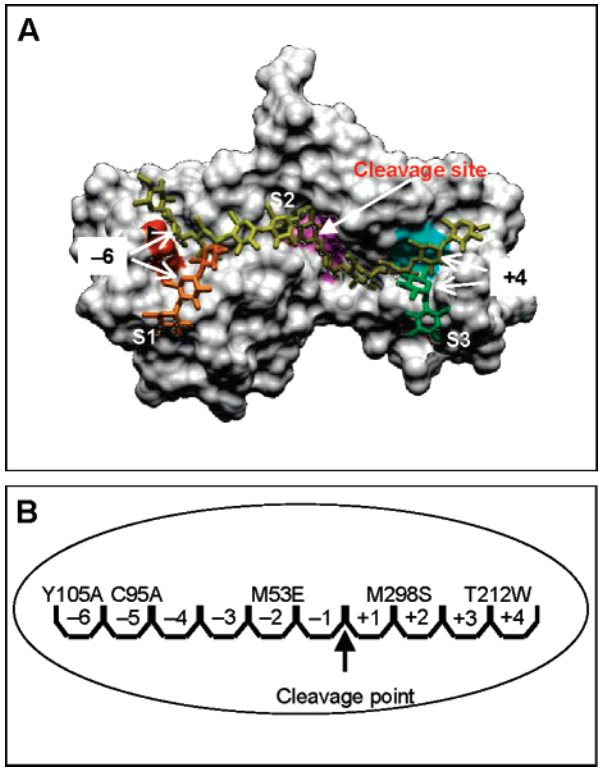

FIGURE 2: (A) Active-site cleft of AMY1. The three-dimensional structure is modeled in complex with maltododecaose. S1, S2, and S3 denotes different docking solutions, of which S1 is favored by polysaccharides (*35*). (B) Schematic outline of the active site of AMY1 with the 10 known subsites. The amino acid replacements are indicated above the modified subsites.

state, a β-D-ester intermediate is formed between C1 of the reducing end residue and the carboxylic group of the catalytic nucleophile. The aglycon part of the substrate is thus free to dissociate. A water molecule, activated by the base form of the catalytic acid, subsequently attacks the ester at C1, resulting in release of the glycon product of the original substrate with retention of the anomeric configuration. In multiple attack by α-amylase, the glycone product is envisaged to reposition in the substrate binding site without dissociating prior to the succeeding hydrolytic attack on a glycoside bond (*8*, *27*). Such sliding is assumed to be controlled by protein dynamics involving breaking and reestablishing of hydrogen bonds, van der Waal contacts, and stacking interactions with aromatic side chains (*7*, *8*). The motion may have features in common with the translocation in maltoporin of maltodextrins, which maintain their helical conformation and move in a screwlike manner through the pore (*28*). In contrast, retaining chitinases (*29*) and presumably also pectinases (*6*), like α-amylases, act on the glycon product after initial cleavage of substrate, and multiple attack, combined with the exo action on the nonreducing end of substrate by the inverting Cel6A cellobiohydrolase (*19*) and β-amylase (*30*), both involve sliding of the aglycon product.

Barley α-amylase contains 10 consecutive glucosyl binding subsites −6 through +4 as determined by subsite mapping, the cleavage occurring between subsites −1 and +1 (*25*, Figure 2). The individual subsite binding energies are comparable (*25*) in isozymes AMY1 and AMY2, having 80% sequence identity (*31*) and very similar three-dimensional structures (*15*, *32*, *33*). High affinity is associated in

AMY1 with subsites −6, −5, −4, −2, +1, +2, and +4 (*25*). Mutational analysis, combined with molecular modeling of maltodextrin (*18*, *34*, *35*), proposed that stacking of substrate glucose onto $Tyr105_{AMY1}$ contributes to the high affinity at subsite −6. The other high-affinity subsites also have characteristic protein−sugar stacking and van der Waals contacts (*18*, *34*, *35*), and the importance of these interactions in hydrolysis of different substrates was addressed by mutations at subsites −5/−6 and +1/+2 (*36*). Finally, hydrogen bonding and stacking to substrate by $Tyr211_{AMY2}$ at subsites +3 and +4 motivated mutations of the corresponding $Thr212_{AMY1}$ to Trp and Tyr (*35*). Previous results showed that these variants all possess strongly modified properties compared to wild type in hydrolysis of different substrates (*23*, *35*, *36*−*38*). This detailed insight into the structure and role of individual AMY1 subsites in the action on the different substrates (*23*, *25*, *35*, *36*, *39*, *40*) prompted the characterization of the impact of the mutant series on DMA. The present study includes the C-terminal AMY1−SBD (starch-binding domain) fusion (*37*) as an example of a polysaccharide hydrolase with several substrate-binding domains (*22*, *41*). The SBD (*42*) contains two starch-binding sites (*43*), and AMY1−SBD thus represents a different way to manipulate polysaccharide binding in AMY1 than by subsite mutation. Certain GH13 members, including AMY1 and AMY2, possess sugar-binding sites situated outside the binding cleft, on the surface of the catalytic domain (*15*, *44*, *45*). In the interaction with polymeric substrates, such sites as well as SBDs might play important roles, for example, in feeding the substrate chain to the active-site crevice and/or by anchoring of enzyme to substrate. Finally, amylose, a water-soluble, polymeric substrate of α-amylase, offers an excellent possibility to quantify the composition of soluble products and analyze DMA in parallel, as opposed to, for example, the degradation of insoluble cellulose by cellulases.

MATERIALS AND METHODS

Materials. AMY1 wild-type (*35*, *40*), Y105A, T212W, Y105A/T212W (*35*), AMY1Δ9 wild-type, M53E (*23*), C95A, and M298S (*36*) were produced in *Pichia pastoris* and purified from culture supernatants by affinity chromatography on β-cyclodextrin−Sepharose as described (*35*, *40*). M53E, C95A, and M298S AMY1 were Δ9 forms lacking the C-terminal nonapeptide of full-length AMY1. Wild type, M53E, and M298S were freed by anion-exchange chromatography from the inactive glutathionylated Cys95 forms representing roughly 25% of the protein (*23*, *36*). AMY1−SBD has a 146-residue C-terminal extension containing part of the O-glycosylated linker and the SBD of *Aspergillus niger* glucoamylase. The fusion protein was produced by heterologous expression in *A. niger* and purified from the culture supernatant (*37*). Protein concentrations were calculated from amino acid contents (Amersham Biosciences/LKB Alpha Plus amino acid analyzer) in hydrolysates as previously described (*35*). Porcine pancreatic α-amylase type I-A was purchased from Sigma.

Different batches of amylose type III from potato (Sigma), originally termed amylose DP440 (*36*), were found to have DP in the range 300−440 based on total carbohydrate determinations by the phenol sulfuric acid method (*46*) and measurements of reducing value of ethanol precipitates. The amylose was dissolved in DMSO (30 min, ambient temperature), and 20 mM sodium acetate and 5 mM $CaCl_2$, pH 5.5, was added. DMA and oligosaccharide product profiles were determined at a final DMSO concentration of 2% and kinetic parameters at 4% DMSO. The DMSO did not affect enzyme activity. Traces of G1−G4 with reducing power equivalent to 4−10 μg (mg of maltose)$^{-1}$ in the different amylose DP440 batches did not affect the enzymatic hydrolysis of amylose (*25*).

Determination of DMA. Amylose solution (1 mg mL^{-1}, 10−15 mL, see above) was equilibrated at 37 °C, and enzyme (0.1−0.8 nM) was added at time zero. Aliquots (1 mL) were removed at time intervals (5−10 min) during the initial stage of hydrolysis and added to 1 M TCA (100 μL) for DMA analysis according to the principle of Robyt and French (*2*). Progress of substrate degradation was assessed by loss in iodine "blue value" (absorbance at 620 nm) for reaction mixture aliquots (50 μL), diluted in water (450 μL) as measured after addition of 0.2% I_2 in 2% KI (500 μL). The remaining mixture was neutralized (0.5 M NaOH, pH indicator paper), and polysaccharide (in 650 μL) was precipitated by 99.9% ethanol (1.3 mL). After 24−48 h at 4 °C, the precipitate was centrifuged (16000*g*, 5 min), washed three times with ethanol (*2*), air-dried, redissolved in DMSO (20 μL, 30 min), and diluted with water (630 μL). The reducing power of the polysaccharide fraction was determined by the copper−bicinchoninate method with maltose (6−29 μg mL^{-1}) as standard (*47*). The total reducing power of the reaction mixture was determined on the remaining pH-adjusted sample diluted with 2 volumes of water. To the maltose standards was added TCA, NaOH, or DMSO to mimic samples. The absorbance of aliquots (300 μL) was measured at 540 nm in a micro plate reader (MRX Revelation, Dynex Technologies). The rates of reducing power formation in the total digest (RV_t) and the polysaccharide fraction (RV_p) were obtained by linear regression analysis of values from 4−6 time points and DMA = (RV_t/RV_p) − 1 was calculated (*2*). The initial stage of amylose hydrolysis is defined as the interval characterized by constant RV_t/RV_p (*2*). Single point measurements of hydrolysis of amylose DP440 by PPA gave, in agreement with previous results (*2*), $RV_t/RV_p = 6.9 \pm 1.6$ (14 determinations) up to ∼20% decrease in iodine blue value. After this stage, RV_t/RV_p increased gradually. DMA of AMY1 wild type and variants was determined over 30−45 min representing 5−20% loss of iodine blue value. In this interval the average DP of the substrate, after a rapid drop to ∼100, slowly decreased to ∼75 (data not shown).

Kinetic Parameters. Initial rates of hydrolysis by the different enzymes (0.8−1.5 nM) were determined at eight amylose concentrations (0.1−2.5 mg mL^{-1}) in 20 mM sodium acetate, 5 mM $CaCl_2$, and 0.005% BSA, pH 5.5, at 37 °C by the copper−bicinchoninate method with maltose as standard (*47*). Kinetic parameters k_{cat} and K_M were calculated by fitting to the Michaelis−Menten equation with the software Curve Expert.

Progress of Oligosaccharide Release. The rates of release from amylose of glucose (G1), oligosaccharides (G2−G7), and short maltodextrins (G8−G10) were obtained by analysis of supernatants from reaction mixtures identical to those used for DMA analysis after inactivation of enzyme by heating (100 °C, 10 min) and precipitation of the polysaccharides as above. The supernatant was vacuum-dried, and the residue

Table 1: Multiple Attack in Hydrolysis of Amylose DP440 by Barley α-Amylase 1 Variants

AMY1 enzyme[a]	subsite localization[b]	RV_t[c] (s^{-1})	RV_p[c] (s^{-1})	RV_s[d] (s^{-1})	DMA[e] $[(RV_t/RV_p) - 1]$
wild-type AMY1		147 ± 33	52 ± 8	95 ± 28	1.9 ± 0.5 (10)
wild-type AMY1Δ9		138 ± 18	48 ± 8	88 ± 15	1.9 ± 0.5 (13)
Y105A	−6	103 ± 18[f]	23 ± 3[f]	78 ± 15	3.3 ± 0.6 (5)[f]
C95A[g]	−5	212 ± 48[f]	80 ± 13[f]	132 ± 45	1.7 ± 0.6 (6)
M53E[g]	−2	70 ± 13[f]	35 ± 5[f]	35 ± 10	1.0 ± 0.2 (6)[f]
M298S[g]	+1/+2	65 ± 7[f]	32 ± 7[f]	33 ± 12	1.2 ± 0.6 (6)[f]
T212W	+4	72 ± 17[f]	30 ± 5[f]	42 ± 13	1.4 ± 0.4 (7)[f]
Y105A/T212W	−6/+4	47 ± 25[f]	22 ± 10[f]	25 ± 16	1.2 ± 0.4 (4)[f]
AMY1−SBD		140 ± 12	37 ± 7[f]	103 ± 10	3.0 ± 0.6 (9)[f]

[a] Enzyme concentrations (nanomolar): wild-type, 0.1−0.3; wild-type Δ9, 0.1; Y105A, 0.4; C95A, 0.1; M53E, 0.4−0.8; M298S, 0.1−0.2; T212W, 0.2−0.3; Y105A/T212W, 0.5−0.8; AMY1−SBD, 0.1−0.3. [b] References *23*, *35*, and *36*. [c] Calculated from rates of reducing value formation (see Materials and Methods). [d] RV_s is calculated as $RV_t - RV_p$. [e] Values of DMA are means ± SD calculated from the linear rates of reducing value formation in each individual experiment, the number of which is given in parentheses. [f] Values significantly different from wild-type values. RV_t values: $P = 0.02$ for Y105A (Student's *t*-test) and $< 1 \times 10^{-4}$ for the other variants. RV_p values: $P < 4 \times 10^{-4}$ for all enzymes. DMA values: $P = 0.02$ and $= 0.03$ for M298S and T212W, respectively, and $< 8 \times 10^{-3}$ for the other variants. [g] M298S, C95A, and M53E are Δ9 forms (see Materials and Methods).

was redissolved in water (100 or 200 μL) and injected (15−25 μL) for HPAEC−PAD (Dionex system, PA100 column). G1−G25 were eluted with a 0−300 mM sodium acetate gradient (5 mM min^{-1}) in 100 mM NaOH at 0.8 mL min^{-1}. G1−G7 were quantified by use of a standard mixture (20 μM each component), and rates of accumulation of the individual products were determined by linear regression analysis of values from 5−7 time points. The G8−G10 accumulation was described by linear rates of increase in peak areas and calculated relative to values from parallel wild-type digests.

Statistical Evaluation. Results were evaluated statistically by the Student's *t*-test (two-sample equal variance). Data sets are considered significantly different for $P \leq 0.05$. *P* values are given in the footnotes to the tables.

RESULTS AND DISCUSSION

DMA of AMY1 Variants. DMA of different α-amylases was originally resolved by Robyt and French (*2*) using the ratio of the reducing power of all products to that of the polysaccharide fraction, as determined for a few samples removed at the early stage of hydrolysis of amylose DP1000. This procedure required prepurification of substrate to remove low molecular weight carbohydrate prior to analysis (*2*). A DMA of ∼1 for barley α-amylase was initially obtained from single-point measurements with a commercial pure amylose (*9*). The present study reports an improved method of DMA analysis that involves monitoring of *rates* of formation of reducing power rather than analysis from individual time points. This procedure permits detection of small changes in DMA and does not require prepurification of the substrate.

Barley wild-type AMY1 and AMY1Δ9 both hydrolyze amylose by a multiple attack mechanism with a DMA of 1.9 ± 0.5 (Table 1); that is, 2.9 glycoside bonds on average are cleaved per productive enzyme−substrate encounter. Thus, after the first bond is hydrolyzed, the substrate repositions in the binding cleft to undergo approximately two more attacks prior to dissociation from the enzyme (*2*, *8*, *48*). Multiple attack was previously shown for PPA acting on ^{14}C-end-labeled maltooctaose to proceed toward the nonreducing end of the substrate (*49*). In accordance with covalent binding of the glycon product after substrate cleavage, reaccommodation of the segment containing the new reducing end at aglycon binding subsites is a requirement for the subsequent (i.e., multiple) attacks to occur (*20*).

The present work confirms that structural changes along the 10-subsite-long binding site in AMY1 affect the DMA in general. DMA thus varied from 1.0 to 3.3 for six AMY1 variants mutated at designated specific substrate binding subsites (Figure 2); Y105A at subsite −6; C95A at subsite −5; M53E at subsite −2; M298S at subsite +1/+2; T212W at subsite +4; and a double mutant Y105A/T212W (Table 1).

Y105A had an increased DMA of 3.3; that is, about four glycosidic bond cleavages took place in a single productive enzyme−substrate complex. For Y105A with modified subsite −6, looser subsite binding was obtained by elimination of Tyr105 stacking onto substrate (Figure 2; *18*, *35*). Thus substrate, despite the reduced apparent affinity (increased K_M) observed in kinetics analysis (see below, Table 2), once it is bound seems to reposition more readily on the variant than on wild-type AMY1. This is consistent with the decreased rate of formation of new reducing polysaccharides (RV_p in Table 1). Maltododecaose complexes have been computed to suggest different binding modes for oligosaccharide and polysaccharide in AMY1 (S2 and S1, respectively, in Figure 2). Moreover, a recent thorough mutational analysis of subsite −6 suggested that insoluble starch employs different binding modes to different extents in Y105A and in wild-type AMY1 (*35*), presumably involving interactions at areas outside the active-site cleft (*13*, *44*). Two such binding sites in AMY1 contain Trp278−Trp279, at the early-recognized starch-binding surface site (*45*), and Tyr380 at a site discovered recently in domain C by crystallography (*44*). Preliminary characterization of Tyr380 mutants, however, indicates that this residue is not important in multiple attack on amylose DP440 (Bozonnet et al., unpublished work).

C95A had a similar DMA as wild-type AMY1, suggesting that subsite −5 is not important for reaccommodation of amylose in the catalytic cleft. The other subsite mutants showed reduced multiple attack. Amino acid substitutions at subsites −2 (M53E) and +1/+2 (M298S) close to the site of catalysis (Figure 2) caused the largest decrease in DMA, to 1.0 and 1.2, respectively (Table 1), implying a

Table 2: Kinetic Parameters for Hydrolysis of Amylose DP440 by Barley α-Amylase 1 Variants

substrate AMY1 enzyme[b]	amylose DP440 k_{cat} (s^{-1})	amylose DP440 K_M (mg mL^{-1})	amylose DP440 k_{cat}/K_M (s^{-1} mg^{-1} mL^{-1})	amylose DP17[a] k_{cat} (s^{-1})	amylose DP17[a] K_M (mg mL^{-1})	amylose DP17[a] k_{cat}/K_M (s^{-1} mg^{-1} mL^{-1})
wild-type AMY1	195 ± 24	0.19 ± 0.04	1026	165 ± 8	0.57 ± 0.09	289 (*35*)
wild-type AMY1Δ9[c]	185 ± 20	0.19 ± 0.01	972	248 ± 16	0.52 ± 0.01	476 (*23*, *36*)
Y105A	178 ± 12	1.4 ± 0.1[d]	132	146 ± 15	2.4 ± 0.7	62 (*35*)
C95A[e]	250 ± 42	0.63 ± 0.18[d]	397	351 ± 16	2.5 ± 0.22	140 (*36*)
M53E[e]	233 ± 12	1.2 ± 0.3[d]	203	208 ± 34	8.0 ± 1.8	26 (*23*)
M298S[c,e]	124 ± 5	0.13 ± 0.02[d]	939	189 ± 16	0.53 ± 0.06	357 (*36*)
T212W	106 ± 1[d]	0.07 ± 0.04[d]	1514	154 ± 6	0.29 ± 0.03	531 (*35*)
Y105A/T212W	134 ± 13[d]	0.27 ± 0.07	496	105 ± 15	2.0 ± 0.09	53 (*35*)
AMY1−SBD	209 ± 36	0.23 ± 0.04	909	225 ± 18	0.45 ± 0.04	560 (*37*)

[a] References to the DP17 data. [b] Enzyme concentrations (nanomolar): wild-type, 0.8−0.9; Y105A, 1.6−1.7; C95A, 0.9; M53E, 0.9−1.6; M298S, 0.5−1; T212W, 0.7−0.9; Y105A/T212W, 0.8−0.9, and AMY1−SBD, 1.4−1.5. Values are means ± SD of three or more individual experiments. [c] Values from ref *36*. [d] Significantly different from wild-type values. $P \leq 0.01$ (Student's *t*-test). [e] M298S, M53E, and C95A are Δ9 forms (see Materials and Methods).

crucial role in multiple attack of the subsites −2 and +1. Subsite −2 has very high affinity in wild-type AMY1 and therefore the low apparent affinity of the M53E mutant (see Table 2) was anticipated to adversely influence repeated substrate sliding, because productive enzyme−substrate complexes will be less stabilized, due to fewer subsites providing efficient contact to substrate (*23*). The replacement M298S enlarges the space at subsite +1/+2 (*36*). This might locally weaken binding and thus limit the number of new aglycon segment accommodation possibilities, despite the slightly reduced K_M and retained transition-state stabilization by this enzyme for amylose DP440 (*36*; see also Table 2).

T212W at subsite +4 had a reduced DMA of 1.4, and the double mutant enzyme Y105A/T212W, involving both outer subsites −6 and +4, had a DMA of 1.2 (Table 1). T212W was made to establish substrate stacking at subsite +4 (*35*). The mutation accordingly resulted in a 3-fold improvement of the apparent substrate affinity (reduced K_M, Table 2). Repositioning of substrate without dissociation was apparently counteracted and substrate sliding into the aglycon binding area was less efficient, probably due to difficulty in accommodating the stable left-hand helical substrate conformation in T212W AMY1 (*35*), thereby leading to fewer repeated attacks. As the double mutant enzyme Y105A/T212W had a low DMA of 1.2, the change in the +4 subsite dominated over loss of stacking at subsite −6, seen in Y105A to increase DMA to 3.3. This may also be inferred from the observation that the subsites −6/+4 double mutant produced insoluble products (RV_p) at the same reduced rate as Y105A and T212W but soluble products at an even lower rate than T212W (Table 1). This strongly indicates that a critical point in the multiple attack mechanism is for the substrate to get efficient binding of the repositioned substrate aglycon part and, moreover, that coordination of substrate chain binding to span the entire binding cleft is delicate and appears to be fully developed only for wild-type AMY1.

AMY1−SBD has the SBD from *A. niger* fused to the C-terminus of AMY1, introducing two additional starch-binding sites from the SBD (*42*) and causing DMA to increase to 3.0 (Table 1) while retaining similar K_M on amylose DP440 as AMY1 (Table 2). AMY1−SBD also showed increased activity toward starch granules (*37*). Possibly, different AMY1−SBD substrate complexes and/or longer residence time of the enzyme on the polysaccharide explain the increase in DMA. The latter point is supported by the decreased rate of formation solely of reducing equivalents in the polysaccharide fraction (Table 1). The high DMA of 6 for PPA having at least one binding site outside the active site (*16*, *24*) supports the possibility of secondary substrate binding sites playing a positive role in multiple attack. Furthermore, this phenomenon is reminiscent of cellulose binding domains in cellulases, where removal of the binding domain from *T. fusca* cellulase reduced the processivity from 7 to a single attack (*5*).

It may be envisaged that the increase in DMA for AMY1−SBD occurs because enzyme and substrate remain associated only by binding at the SBD. In this case the catalytic site would be free to hydrolyze substrate in the vicinity of the primary attack, which would resemble multiple attack but not involve sliding. Such a mechanism cannot be ruled out on the basis of the present data and may in fact be included as a type of multiple attack.

Except for C95A, which had increased product release rates, all subsite variants, irrespective of the DMA, actually had decreased rates of insoluble product formation (RV_p) compared to wild-type AMY1. Reduced RV_p may thus arise either from an increased tendency of substrate repositioning without dissociation, as discussed above for the variants with increased DMA, or from looser binding and increased tendency to dissociate, as for the variants of reduced DMA. Soluble product formation (RV_s), however, was only moderately reduced and unchanged, respectively, for Y105A and AMY1−SBD, as reflected in the increased DMA of these variants. The subsite mutant enzymes with low DMA all reduced RV_s to a larger extent than RV_p (Table 1). To further characterize the mutant enzymes and the AMY1−SBD fusion with respect to enzyme−substrate interactions, k_{cat} and K_M were assessed for amylose DP440 hydrolysis and the progress of release of individual oligosaccharides was investigated.

Kinetics of Hydrolysis of Amylose DP440. The soluble, linear polysaccharide amylose DP440 is distinguished from the previously used routine substrates by having a much larger DP. Qualitatively very similar but, for some mutant enzymes, more pronounced effects than with amylose DP17 were observed for the DP440 (Table 2). Y105A/T212W had K_M similar to wild type and hence intermediate to the values of the corresponding single AMY1 mutants. Interestingly, K_M of Y105A/ T212W was increased only for amylose DP17, whereas Y105A maintained decreased apparent affinity for

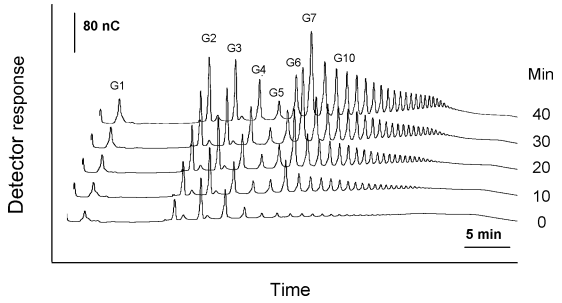

FIGURE 3: Oligosaccharides released during the initial stage of amylose hydrolysis by wild-type AMY1 (0.2 nM) The oligosaccharides formed were separated from polysaccharides by ethanol precipitation and chromatographed by HPAEC−PAD (see Materials and Methods). The products at 40 min represent 19% substrate degradation as estimated from the decrease in iodine blue value (A_{620}).

both amylose DP17 and DP440, confirming a dominant role of the T212W replacement on the action toward the longer substrate. The k_{cat} differences are expected to mirror RV_t (Table 1). This indeed was essentially the case except for Y105A and M53E AMY1, where RV_t was more reduced than k_{cat} compared to wild-type AMY1. This was a consequence of RV_t being measured at nonsaturating conditions (1 mg mL^{-1} amylose DP440) as indicated by the K_M of these variants (Table 2). The k_{cat} for T212W was 55% that of wild-type enzyme but was only marginally affected for the other variant enzymes; M298S and the double mutant both showed a k_{cat} ~70% that of wild-type AMY1 (Table 2). Thus, changes in the catalytic efficiency (k_{cat}/K_M) were mostly due to an effect on K_M, with the largest effects seen for T212W, with k_{cat}/K_M augmented by 50%, and Y105A, with k_{cat}/K_M decreased to about 13% (Table 2). The k_{cat} values for amylose DP440 essentially match the activities on insoluble blue starch (*23*, *36*, *50*). Exceptions were Y105A and the double mutant enzyme Y105A/T212W, which had unchanged and decreased k_{cat}, respectively, on amylose DP440 but increased activity on blue starch (*50*). This marked difference between the soluble and insoluble substrates was also seen with amylose DP17 (*35*) and was explained to be a result of the absence of the stacking possibility at subsite −6 in both Y105A and the double mutant enzyme, showing adverse effects on the binding of soluble substrates (*35*). It should be noted that k_{cat} cannot be directly correlated to the degree of multiple attack because k_{cat} reflects the combined result of the independent events: (i) the rate of release of the product in each catalytic event, (ii) the rate of each substrate repositioning, (iii) the number of repeated repositions, and (iv) the rate of dissociation of substrate from the enzyme. Finally, the observation that the long substrate amylose DP440 in general is a better substrate than amylose DP17 may be attributed to the use of binding sites outside the catalytic cleft (*44*, *45*), which somehow could compensate for adverse effects of the subsite mutations.

Oligosaccharide Product Profiles from Amylose Hydrolysis. DMA involves consecutive formation of relatively short products from polysaccharide substrates. Supernatants after ethanol precipitation of amylose digested by barley α-amylase contain glucose, maltooligosaccharides, and maltodextrins up to ~DP25 in the initial stage of hydrolysis as deduced from ~25 peaks appearing in HPAEC−PAD (Figure 3). G2 and G6−G10 were major initial products of wild-type enzyme and most of the AMY1 variants (Table 3), but despite the complex soluble product composition, similarities as well as distinct differences among the variants could be identified.

Rates of G1−G7 Release. G7 was produced at the highest rate in all cases (Table 3). Y105A, C95A, and AMY1−SBD produced G7 at rates essentially similar to wild type, whereas M53E, M298S, T212W, and Y105A/T212W AMY1 produced G7 more slowly, as also expected from the RV_s values (Table 1). However, since the results all were obtained with 1 mg mL^{-1} amylose DP440, it is likely that the overall soluble product release would be higher for Y105A, C95A, and M53E if it was determined at substrate concentrations well above K_M as in the case of the other variants. Despite this, significant differences among the variants were observed (Table 3). Most remarkably, all subsite mutant enzymes produced G1 at a much slower rate than wild-type AMY1. It follows that the ability to reposition the terminal glucose unit of the substrate to subsite +1 seemed to be lost in the subsite variants. The complete loss of detectable G1 production for Y105A and C95A situated at outer glycon subsites may stem from the reduced apparent affinity (increased K_M, Table 2) for substrate that facilitates interaction at the aglycon binding subsites, shifting the balance between glycon and aglycon accommodation. For M53E and M298S, the reduced G1 production rate may result from altered binding in the close proximity to subsite +1 (*20*, *23*, *36*). Replacing Thr212 by Trp in the T212W enzyme, affecting subsites +3 and +4 (*35*), resulted in the only subsite variant, except C95A, that produced G2 at a rate comparable to wild-type enzyme. This mutation perhaps suppressed the short-distance sliding of the reducing-end glycosyl ring beyond subsite +2. The increase in apparent affinity (Table 2), caused by the introduced aromatic group, was accompanied by disappearance of the products G3 and G4, which could reflect promoted binding at outer subsites, possibly in the S3 binding mode as suggested previously (see ref *35*). This indicates that this binding mode could be less prone to multiple attack than the S1 binding mode which most probably is preferred by barley α-amylase in hydrolysis of polysaccharides (Figure 2A; *35*). M53E had low formation rates of all soluble products, especially of G1−G5. This may, at least in part, be due to the experiments with M53E being performed at a substrate concentration below K_M as pointed out above. For M298S all products except G3 were formed at slower rates than for the wild-type enzyme. The fusion AMY1−SBD that has two extra substrate binding sites on the SBD (*43*) produced G3 and G4 at reduced rates compared to wild-type AMY1. This, however, was apparently accompanied by improved accommodation of longer substrate aglycon segments in the multiple attacks as indicated by relatively increased rates of production of G8−G10 (see below and Figure 4B). For all enzymes G5 was a minor product (Table 3).

The initial rates of production of G8 and G10 by Y105A were 1.5- and 1.3-fold higher, respectively, than obtained for the wild-type AMY1. Also, C95A tended to produce G8−G10 at somewhat increased rates (~1.2-fold). M53E at subsite −2 and the double mutant Y105A/T212W, in contrast, produced G8−G10 at rates 50% that of wild type, while the other variant enzymes produced G8−G10 at rates similar to wild type (data not shown).

Table 3: Rates of Production of G1−G7 during the Initial Phase of Degradation of Amylose DP440

AMY1 enzyme[a]	subsite	G1 (s^{-1})	G2 (s^{-1})	G3 (s^{-1})	G4 (s^{-1})	G5 (s^{-1})	G6 (s^{-1})	G7 (s^{-1})
wild-type AMY1		2.9 ± 0.8	7.0 ± 2.6	2.9 ± 1.1	2.0 ± 0.9	1.0 ± 0.5	6.9 ± 1.8	18.3 ± 3.7
Y105A	−6	0[b]	2.5 ± 1.0[b]	1.5 ± 0.5[b]	1.9 ± 0.9	1.1 ± 0.5	6.2 ± 1.8	19.0 ± 5.1
C95A[c]	−5	0[b]	4.0 ± 0.8[d]	3.0 ± 0.6	2.1 ± 0.7	1.5 ± 0.5	9.0 ± 1.8[d]	23.4 ± 6.0
M53E[c]	−2	0.2 ± 0.3[b]	0.8 ± 0.7[b]	0.5 ± 0.8[b]	0.7 ± 0.1[b]	0.2 ± 0.4[b]	3.0 ± 0.6[b]	10.9 ± 3.4[b]
M298S[c]	+1/+2	0.2 ± 0.3[b]	2.5 ± 0.5[b]	2.9 ± 0.4	1.2 ± 0.3	0.7 ± 0.2	3.6 ± 0.6[b]	13.2 ± 2.7[b]
T212W	+4	1.0 ± 0.3[b]	5.1 ± 0.8	0[b]	0[b]	0.7 ± 0.2	4.8 ± 0.8[b]	12.0 ± 3.2[b]
Y105A/T212W	−6 and +4	0.3 ± 0.2[b]	1.0 ± 0.8[b]	0.7 ± 0.4[b]	1.0 ± 0.4[b]	0.6 ± 0.4	4.0 ± 0.7[b]	10.2 ± 0.7[b]
AMY1−SBD		3.2 ± 0.5	6.1 ± 2.9	1.3 ± 0.9[b]	0.3 ± 0.3[b]	0.8 ± 0.6	8.9 ± 1.4[d]	22.0 ± 2.1

[a] Enzyme concentration (nanomolar): wild-type, 0.1−0.4; Y105A, 0.1−0.2; C95A, 0.2−0.25; M53E, 0.2; M298S, 0.3−0.4; T212W, 0.25−0.3; Y105A/T212W, 0.3−0.6; and AMY1−SBD, 0.15−0.2. The values are mean ± SD of 12 independent experiments for wild-type, 5 for Y105A and M298S, 4 for T212W, Y105A/T212W, and AMY1−SBD, and 3 for C95A and M53E. [b] Value significantly different from wild-type value. $P = 0.05$ for release of G6 by T212W. In all other cases $0 \leq P \leq 0.04$. [d] $P = 0.09$. [c] C95A, M53E, and M298S are Δ9 forms.

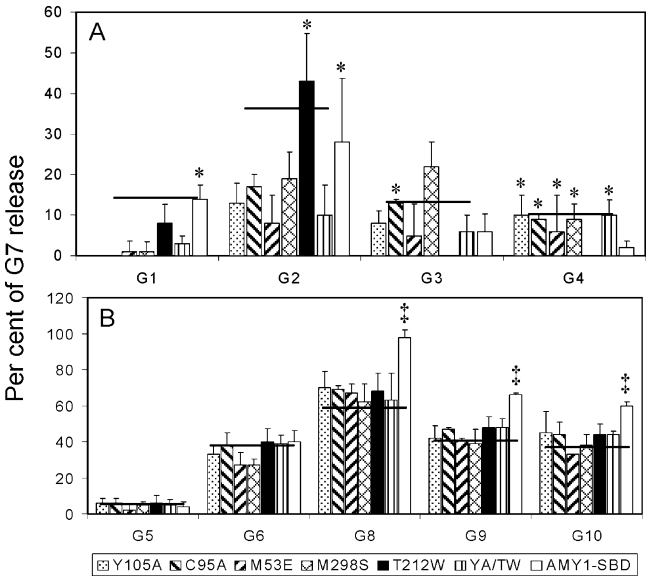

FIGURE 4: (A) Rates of production of glucose (G1) and the maltooligosaccharides G2−G4, normalized by the rates of G7 release = 100. *Values *not* significantly different from wild type. Significantly different values gave $P \leq 0.01$ (Student's *t*-test) except for M298S, where $P = 0.03$. (B) As above for G5, G6, and G8−G10. The relative rates of release for G8−G10 were calculated from the respective rates of area increase normalized to the G7-area increase rate. ‡Values significantly *different* from wild type. $P \leq 4 \times 10^{-6}$ (Student's *t*-test). For both panels: vertical bars show the standard deviation and horizontal bars show the corresponding relative rates for wild-type AMY1.

Barley α-amylase was previously reported not to hydrolyze maltododecaose by multiple attack (*48*, *51*). This is in contrast to multiple attack being demonstrated for PPA also for even shorter substrates (*24*). The preferred sliding distance of barley α-amylase corresponds to seven glucose residues, as G7 was found to be the major product at initial hydrolysis of amylose (Table 3; *48*, *51*). Assuming that the outermost subsites, as suggested previously, play a major role in the initial stage of substrate binding to barley α-amylase (*18*, *48*), maltododecaose is too short to be hydrolyzed by a multiple attack mechanism producing G7.

Product Release Profiles. To facilitate comparison of the different AMY1 variants with respect to initial product formation, the production rates of G1−G6 (Table 3) were normalized to that of the G7 production rate for each AMY1 variant (Figure 4). In addition, to cover all 10 subsites of the substrate-binding site, the area increase rates for each of the G7−G10 peaks were used to normalize the production rates of G8, G9, and G10 to that of G7 (Figure 4B). Wild-type AMY1 thus produced G1 through G6 at rates from 5% (G5) to 38% (G2 and G6) of the G7 production rate (Figure 4). The variants produced shorter products, especially G1−G3, at highly varying relative rates (Figure 4A), and G4 was produced at 6−11% the rate of G7 release by wild type and most variants, except for the complete lack of detection and low production in the case of T212W and AMY1−SBD, respectively. Noticeably, among the short products only G1 by AMY1−SBD, G2 by T212W and AMY1−SBD, and G3 by C95A and M298S were released at relative rates comparable to those of wild type.

Remarkably, the relative rate distribution of G1−G4 for Y105A/T212W resembled more closely that of Y105A than that of T212W despite the lower overall rates of production of oligosaccharides by both T212W and the double mutant enzyme. This is in contrast to the dominating effect of the T212W replacement on (i) DMA, (ii) soluble product formation (Table 1), and (iii) K_M for DP440 (Table 2). It may be speculated that in the double mutant the Y105A mutation determines the product composition, whereas T212W is the determinant of the number of events per enzyme−substrate encounter. Interestingly, the G3 production by M298S was increased relative to G7 compared to wild-type AMY1, whereas G2 production was reduced (Figure 4A). M298S had modified subsites +1/+2, and subsite +3 may thus compensate for loss of interactions close to the catalytic site. Notably, the production rates of G1−G4 relative to the G7 rate by M53E constituted only 20% compared to 80% for wild type and 30−50% for the other AMY1 variants, indicating narrow product specificity for M53E. Narrow product specificity was also observed for T212W AMY1, which produced G2 at a similar relative rate as wild-type AMY1 and had much reduced G1 production and no detectable formation of G3 and G4. For all variant enzymes G5 appeared at 2−6% of the G7 release rate and G6 at 27−40% (Figure 4B).

G8, G9, and G10 appeared at relative rates 62−70%, 39−48%, and 33−45% of the G7 production rate for all the subsite mutant enzymes. This resembles the wild-type enzyme producing G8, G9, and G10 at 60%, 42%, and 38% of the G7 production rate, respectively (Figure 4B). The relative production rates of G5−G10 were thus very similar for the subsite mutant enzymes, indicating marginal impact of subsite structural changes on formation of these products. This is in contrast to the highly diverse distribution of the shorter products G1−G4 (Figure 4A). In clear distinction to the other variants, AMY1−SBD had elevated formation of

G8−G10 relative to the G7 production rate, in particular G8, compared to wild-type AMY1. This behavior suggests that the SBD stabilizes the enzyme−substrate complex and allows longer sliding between successive attacks than wild type (Figure 4B).

Noticeably, G5 and higher oligosaccharides, released in amylose hydrolysis, may serve as substrate for AMY1 and the variants, several of which had rather different action patterns (*23*, *25*, *35*−*38*). It may be thought that especially the shorter products (Table 3, Figure 4A) arose from secondary hydrolytic events on initially formed larger oligosaccharides. However, based on previous action pattern analysis (*23*, *25*, *35*−*38*), secondary hydrolysis of, for example, G7 would generate significant amounts of G5 by all enzymes used here—except M298S (*36*)—but no G5 was formed (Table 3). C95A similarily should release glucose from G7 (*36*), which however was not observed (Table 3). Furthermore, none of the product release plots deviated from linearity during the experimental period. Hence, secondary hydrolysis of oligosaccharides did not contribute to bias of the product profiles or to erroneous DMA values.

The size of the individual oligosaccharide products reflects the length of translocation in the multiple attacks (*8*). Although G7 is the predominant product, a size distribution was obtained, as expected for an enzyme with an extended substrate-binding cleft, allowing a range of products. This agrees with an earlier study on amylose degradation by barley α-amylases yielding a similar oligosaccharide profile with G7 as the dominating product but with G1 as the minor product (*48*). In comparison PPA, having a DMA of 6 and only five subsites (−3 through +2), initially forms only large amounts of G2 and some G3 from amylose (*2*, *52*). In analogy with PPA, AMY1 (subsites −6 through +4) should produce large amounts of G4 and some longer products. This, however, was not observed. Thus the number of aglycon binding subsites did not match the actual oligosaccharide products, perhaps because of the presence of more subsites, which might contribute to processing of longer substrates. Modeling of maltododecaose complexes actually indicates the presence of subsite +5 in AMY2 (*35*). Another possibility is the involvement of binding at surface sites situated outside the substrate-binding cleft (*15*, *18*, *25*, *44*). Such sites, however, would be identical in all AMY1 subsite mutants, although the interplay with the active site might vary for the different mutants.

CONCLUSION

Amylose DP440 was hydrolyzed by AMY1 substrate binding site variants in a multiple attack mechanism. The DMA was sensitive to structural changes in the substrate-binding cleft as well as to introduction of additional binding sites by fusion with SBD. On the basis of the oligosaccharide product profiles, amylose upon the initial hydrolytic attack apparently underwent (i) long-distance sliding regardless of subsite changes leading mainly to G6−G10, reflecting the extended binding site of AMY1, and (ii) shorter sliding, of which both the translocation distance and the frequency varied among the mutants. The observed long-distance sliding implies substrate binding outside the cleft or structural features characteristic of the polysaccharide substrate chain, or both, to be important in amylose hydrolysis. The present results provide new insight into structure−function relationships of barley α-amylase acting on a polymeric substrate with relevance for other polysaccharide-degrading enzymes.

ACKNOWLEDGMENT

Sidsel Ehlers, Annette Gajhede, and Lone Sørensen are thanked for excellent technical assistance and Christina de Castro and Anders Broberg for help with the Dionex system. We are grateful to Gwenaëlle André and Vinh Tran for discussions on modeling of maltodextrin to barley α-amylase and to Martin Willemoës for valuable criticism of the manuscript.

REFERENCES

1. Bailey, J. M., and French, D. (1956) The significance of multiple reactions in enzyme−polymer systems, *J. Biol. Chem. 226*, 1−14.
2. Robyt, J. F., and French, D. (1967) Multiple attack hypothesis of α-amylase action: action of porcine pancreatic, human salivary, and *Aspergillus oryzae* α-amylases, *Arch. Biochem. Biophys. 122*, 8−16.
3. Nakatani, H. (1997) Monte Carlo simulation of multiple attack mechanism of *β*-amylase catalyzed reaction, *Biopolymers 42*, 831−836.
4. French, D. (1981) Amylases: Enzymatic mechanisms, *Basic Life Sci. 18*, 151−182.
5. Irwin, D., Shin, D.-H., Zhang, S., Barr, B. K., Sakon, J., Karplus, P. A., and Wilson, D. B. (1998) Role of the catalytic domain and two cellulose binding domains of *Thermospora fusca* E4 in cellulose hydrolysis, *J. Bacteriol. 180*, 1709−1714.
6. Pagès, S., Kester, H. C. M., Visser, J., and Benen, J. A. E. (2001) Changing a single amino acid residue switches processive and nonprocessive behaviour of *Aspergillus niger* endopolygalacturonase I and II, *J. Biol. Chem. 276*, 33652−33656.
7. Breyer, W. A., and Matthews, B. W. (2001) A structural basis for processivity, *Protein Sci. 10*, 1699−1711.
8. Mazur, A. K., and Nakatani, H. (1993) Multiple attack mechanism in the porcine pancreatic α-amylase hydrolysis of amylose and amylopectin, *Arch. Biochem. Biophys. 306*, 29−38.
9. Kramhøft, B., and Svensson, B. (1998) Effect of temperature and Ca^{2+} on the degree of multiple attack exhibited by mesophilic and thermophilic α-amylases, *Progress in Biotechnology 15*, (Ballasteros, A., Plou, F. J., Iborra, J. L., and Halling, P. J., Eds) pp 343−347, Elsevier, Amsterdam.
10. Irwin, D. C., Spezio, M., Walker, L. P., and Wilson, D. B. (1993) Activity studies of eight purified cellulases: specificity, synergism, and binding domain effects, *Biotechnol. Bioeng. 42*, 1002−1013.
11. Zang, S., Irwin, D. C., and Wilson, D. B. (2000) Site-directed mutation of noncatalytic residues of *Thermobifida fusca* exocellulase Cel6B, *Eur. J. Biochem. 267*, 3101−3115.
12. Uchiyama, T., Katouno, F., Nikaidou, N., Nonaka, T., Sugiyama, J., and Watanabe, T. (2001) Role of the exposed aromatic residues in crystalline chitin hydrolysis by chitinase A from *Serratia marcescens* 2170, *J. Biol. Chem. 276*, 41346−41349.
13. Kadziola, A., Søgård, M., Svensson, B., and Haser, R. (1998) Molecular structure of a barley α-amylase inhibitor complex: implications for starch binding and catalysis, *J. Mol. Biol. 278*, 205−217.
14. Koivula, A., Kinnari, T., Harjunpää, V., Ruohonen, L., Teleman, A., and Teeri, T. T. (1998) Tryptophan 272: an essential determinant of crystalline cellulase degradation by *Trichoderma reesei* cellobiohydrolase Cel6A, *FEBS Lett. 428*, 341−346.
15. Robert, X., Haser, R., Svensson, B., and Aghajari, N. (2002) Comparison of crystal structures of barley α-amylase 1 and 2: implications for isozyme differences in stability and activity, *Biologia 57* (Suppl. 11), 59−70.
16. Koukiekolo, R., Desseaux, V., Moreau, Y., Marchis-Mouren, G., and Santimone, M. (2001) Mechanism of porcine pancreatic alpha-amylase. Inhibition of amylose and maltopentaose hydrolysis by alpha-, beta-, and gamma-cyclodextrins, *Eur. J. Biochem. 268*, 841−848.
17. Ji, Q., Winken, J. P., Suurs, L. C., and Visser, R. G. (2003) Microbial starch-binding domains as a tool for targeting proteins to granules during starch biosynthesis, *Plant Mol. Biol. 51*, 789−801.

18. André, G., Buléon, A., Haser, R., and Tran, V. (1999) Amylose chain behaviour in an interacting context III. Complete occupancy of the barley amylase cleft and comparison with biochemical data, *Biopolymers 50*, 751−762.
19. Varrot, A., Frandsen, T. P., von Ossowski, I., Boyer, V., Cottaz, S., Driguez, H., Schülein, M., and Davies, G. J. (2003) Structural basis of ligand binding and processivity in cellobiohydrolase Cel6A from *Humicola insolens*, *Structure 11*, 855−864.
20. MacGregor, E. A., Janeček, Š., and Svensson, B. (2001) Relationship of sequence and structure to specificity in the α-amylase family of enzymes, *Biochim. Biophys. Acta 1546*, 1−20.
21. Henrissat, B., and Coutinho, P. M. Carbohydrate active enzymes, http://afmb.cnrs-mrs.fr/CAZY/index.html.
22. Janeček, Š. (2000) Structural features and evolutionary relationships in the alpha-amylase family, in *Glycoenzymes* (Ohnishi, M., Aayashi, T., Ishima, S., and Kuriki, T., Eds) pp 19−54, The Japanese Scientific Societies Press, Tokyo.
23. Mori, H., Bak-Jensen, K. S., and Svensson, B. (2002) Barley α-amylase Met53 situated at the high-affinity subsite −2 belongs to a substrate binding motif in the $\beta\rightarrow\alpha$ loop 2 of the catalytic $(\beta/\alpha)_8$-barrel and is critical for activity and substrate specificity, *Eur. J. Biochem. 269*, 5377−5390.
24. Robyt, J. F., and French, D. (1970) The action pattern of porcine pancreatic α-amylase in relationship to the substrate binding site of the enzyme, *J. Biol. Chem. 245*, 3917−3927.
25. Ajandouz, E. H., Abe, J., Svensson, B., and Marchis-Mouren, G. (1992) Barley malt α-amylase. Purification, action pattern and subsite mapping of isozyme 1 and two members of the isozyme 2 subfamily using *p*-nitrophenylated maltooligosaccharide substrates, *Biochim. Biophys. Acta 1159*, 193−202.
26. Kandra, L., Gyémánt, G, Remenyik, J., Hovánski, G., and Lipták, A. (2002) Action pattern and subsite mapping of *Bacillus licheniformis* α-amylase (BLA) with modified maltooligosaccharide substrates, *FEBS Lett. 518*, 79−82.
27. Petukhov, M. G., and Mazur, K. (1992) Modelling of possible methods of substrate binding in the active site of α-amylase from *Aspergillus oryzae*, *Mol. Biol. 26*, 292−299.
28. Dutzler, R., Schirmer, T., Karplus, M., and Fischer, S. (2002) Translocation mechanism of long sugar chains across the maltoporin membrane channel, *Structure 10*, 1273−1284.
29. Uchiyama, T., Katouno, F., Nikaidou, N., Nonaka, T., Sugiyama, J., and Watanabe, T. (2001) Roles of exposed aromatic residues in crystalline chitin hydrolysis by chitinase A from *Serratia marcescens* 2170, *J. Biol. Chem. 276*, 41343−41349.
30. Adachi, M., Mikami, B., Katsube, T., and Utsumi, S. (1998) Crystal structure of recombinant soybean β-amylase complexed with β-cyclodextrin, *J. Biol. Chem. 273*, 19859−19865.
31. Svensson, B., Mundy, J., Gibson, R. M., and Svendsen, I. (1985) Partial amino acid sequences of α-amylase isozymes from barley malt, *Carlsberg Res. Commun. 50*, 15−22.
32. Kadziola, A., Abe, J., Svensson, B., and Haser, R. (1994) Crystal and molecular structure of barley α-amylase, *J. Mol. Biol. 239*, 104−31.
33. Robert, X., Gottschalk, T. E., Haser, R., Svensson, B., and Aghajari, N. (2002) Expression, purification and preliminary crystallographic studies of alpha-amylase isozyme 1 from barley seeds, *Acta Crystallogr. D: Biol. Crystallogr. 58*, 683−686.
34. André, G., and Tran, V. (1999) Molecular modelling of complexes between α-amylases and amylose fragments of high DP, in *Recent Advances in Carbohydrate Bioengineering* (Gilbert, H. J., Davies, G. J., Henrissat, B., and Svensson, B., Eds) pp 165−175, Royal Society of Chemistry, London.
35. Bak-Jensen, K. S., André, G., Gottschalk, T. E., Päes, G., Tran, V., and Svensson, B. (2004) Tyrosine 105 and Threonine 212 at outermost substrate binding subsites −6 and +4 control substrate specificity, oligosaccharide cleavage patterns, and multiple binding modes of barley α-amylase 1, *J. Biol. Chem. 279*, 10093−10102.
36. Mori, H., Bak-Jensen, K. S., Gottschalk, T. E., Motawia, M. S., Damager, I., Møller, B. L., and Svensson, B. (2001) Modulation of activity and substrate binding modes by mutation of single and double subsites +1/+2 and −5/−6, *Eur. J. Biochem. 268*, 6545−6558.
37. Juge, N., Le Gal-Coëffet, M.-F., Furniss, C. S. M., Gunning, A. P., Kramhøft, B., Morris, V. J., Williamson, G., and Svensson, B. (2002) The starch binding domain of glucoamylase from *Aspergillus niger*: an overview of its structure, function, and role in raw starch hydrolysis, *Biologica 57* (Suppl. 11), 230−245.
38. Matsui, I., and Svensson, B. (1997) Improved activity and modulated action pattern obtained by random mutagenesis at the fourth $\beta-\alpha$ loop involved in substrate binding to the catalytic $(\beta/\alpha)_8$-barrel domain of barley α-amylase 1, *J. Biol. Chem. 272*, 22456−22436.
39. Gottschalk, T. E., Tull, D., Aghajari, N., Haser, R., and Svensson, B. (2001) Specific modulation of barley α-amylase through biased random mutagenesis involving a conserved tripeptide in $\beta\rightarrow\alpha$ loop 7 of the catalytic $(\beta/\alpha)_8$-barrel domain, *Biochemistry 40*, 12844−12854.
40. Juge, N., Andersen, J. S., Tull, D., Roepstorff, P., and Svensson, B. (1996) Overexpression, purification, and characterization of recombinant barley α-amylases 1 and 2 secreted by the methylotrophic yeast *Pichia pastoris*, *Protein Expression Purif. 8*, 204−214.
41. Coutinho, P. M., and Henrissat, B. (1999) Carbohydrate-active enzymes: an integrated database approach, in *Proceedings of the 3rd Carbohydrate Bioengineering Meeting on Recent Advances in Carbohydrate Bioengineering* (Gilbert, H. J., Davies, G. J., Henrissat, B., and Svensson, B., Eds.) pp 3−12, Royal Society of Chemistry, Cambridge, U.K.
42. Sauer, J., Sigurskjold, B. W., Christensen, U., Frandsen, T. P., Mirgorodskaya, E., Harrison, M., Roepstorff, P., and Svensson, B. (2000) Glucoamylase: structure/function relationship and protein engineering, *Biochim. Biophys. Acta 1543*, 275−293.
43. Le Gal-Coëffet, M.-F., Jacks, A. J., Sorimachi, K., Williamson, M. P., Williamson, G., and Archer, D. B. (1995) Expression in *Aspergillus niger* of the starch binding domain of glucoamylase. Comparison with the proteolytically produced starch binding domain, *Eur. J. Biochem. 233*, 561−567.
44. Robert, X., Haser, R., Gottschalk, T., Ratajczak, F., Driguez, H., Svensson, B., and Aghajari, N. (2003) The structure of barley α-amylase 1 reveals a novel role of domain C in substrate recognition and binding: a pair of sugar tongs, *Structure 11*, 973−984.
45. Søgaard, M., Kadziola, A., Haser, R., and Svensson, B. (1993) Site-directed mutagenesis of histidine 93, aspartic acid 180, glutamic acid 205, histidine 290, and aspartic acid 291 at the active site and tryptophan 279 at the raw starch binding site in barley α-amylase 1, *J. Biol. Chem. 268*, 22480−22484.
46. Chaplin, M. F. (1986) Monosaccharides, In *Carbohydrate analysis, a practical approach* (Chaplin, M. F., and Kennedy, J. F., Eds.) pp 1−36, IRL Press Ltd., Oxford, Washington, DC.
47. McFetters, R. F. (1980) A manual method for reducing sugar determinations with 2,2′-bicinchoninate reagent, *Anal. Biochem. 103*, 302−306.
48. MacGregor, E. A., MacGregor, A. W., Macri, L. J., and Morgan, J. E. (1994) Models for the action of barley alpha-amylase isozymes on linear substrates, *Carbohydr. Res. 257*, 249−268.
49. Robyt, J. F., and French, D. (1970) Multiple attack and polarity of action of porcine α-amylase, *Arch. Biochem. Biophys. 138*, 662−670.
50. Bak-Jensen, K. S. (1999) Protein engineering of the action pattern and the influence of calcium ions and halides on the activity of barley α-amylase 1, M.Sc. Thesis, University of Copenhagen, Denmark.
51. MacGregor, E. A., and MacGregor, A. W. (1985) A model for the action of cereal alpha amylases on amylose, *Carbohydr. Res. 142*, 223−236.
52. Banks, W., Greenwood, C. T., and Khan, K. M. (1970) Studies on starch-degrading enzymes. Part XII. The initial stages of the action on amylose of the alpha-amylases from *B. subtilis*, human saliva, malted rye, and porcine pancreas, *Carbohydr. Res. 12*, 79−87.

BI048100V